Published in final edited form as:
J Inorg Biochem. 2007 November ; 101(11-12): 1768–1775.

Probing the Cytochrome *c′* Folding Landscape

Ekaterina V. Pletneva, **Ziqing Zhao**, **Tetsunari Kimura**, **Krastina V. Petrova**, **Harry B. Gray***, and **Jay R. Winkler***
Beckman Institute, California Institute of Technology, Pasadena, CA 91125

Abstract

The folding kinetics of *R. palustris* cytochrome *c′* (cyt *c′*) have been monitored by heme absorption and native Trp72 fluorescence at pH 5. The Trp72 fluorescence burst signal suggests early compaction of the polypeptide ensemble. Analysis of heme transient absorption spectra reveals deviations from two-state behavior, including a prominent slow phase that is accelerated by the prolyl isomerase cyclophilin. A nonnative proline configuration (Pro21) likely interferes with the formation of the helical bundle surrounding the heme.

Keywords

folding; kinetics; intermediates; singular-value decomposition

Introduction

Many four-helix-bundle proteins [1-3], including cytochrome b_{562} [4], the acyl-CoA binding protein (ACBP) [5], and the *N*-terminal domain of λ repressor [6], fold on the millisecond timescale. In contrast, complete refolding of *R. palustris* cytochrome *c′* (cyt *c′*), which has a covalently bound heme group linked to the polypeptide by an axial histidine (His117) and two thioether bonds at (Cys113 and Cys116) (Fig. 1) [7], takes many seconds [8]. Unfolding is accompanied by large absorption changes as the heme becomes six-coordinate. Time-resolved absorption measurements on the reduced protein revealed highly heterogeneous folding kinetics, possibly indicating that a methionine (Met15 or Met25) can transiently bind to the Fe (II) heme [8]. This scenario is unlikely for the ferric protein, since the affinity of methionine for an Fe(III) heme is low in the denatured state [9].

Our previous efforts have focused primarily on the kinetics of fluorescence energy transfer from native Trp72 or mutant Trp32 to the heme in the ferric protein [2,10]. Analysis of the Trp-to-heme distance distributions revealed substantial populations of compact conformations in the denatured protein as well as nonnative collapsed structures during early stages (~ 150 μs) of refolding. Interestingly, we found that Trp32 appears to approach the heme faster than Trp72, suggesting that folding bottlenecks occur after the development of structure in some parts of the protein [2].

*Corresponding authors. E-mails: hbgray@caltech.edu (H.B.G.) and winklerj@caltech.edu (J.R.W.)..

We dedicate this work to the memory of Ed Stiefel, a great colleague and friend.

Here we report a detailed investigation of ferric cyt *c′* refolding kinetics at pH 5, with particular emphasis on the slower events. Characterization of these processes, which play a critical role in refolding, is essential for elucidation of the nature and origins of deep folding traps. We have monitored the reaction kinetics, including examination of the "burst" phase, both by absorption and Trp72 fluorescence. These data, together with a singular-value decomposition analysis of multiple-wavelength absorbance changes, rule out a two-state folding mechanism and also provide spectroscopic signatures of intermediates trapped in rugged sections of the folding landscape.

Materials and Methods

General

Distilled water was demineralized to a resistivity greater than 18 MΩ•cm. Chromatography resins and prepacked columns were obtained from Amersham Biosciences. Glutathione resin, glutathione, guanidine hydrochloride (GuHCl, SigmaUltra grade), lysozyme, chymotrypsin, and the peptide *N*-succinyl-Ala-Ala-Pro-Phe-*p*-nitroanilide were from Sigma Chemical Co. All other chemicals were obtained from Mallinckrodt Baker, Inc. All folding experiments were performed in a 100 mM sodium acetate (NaOAc) buffer at pH 5.0±0.2 at 18 °C, unless specified otherwise.

Cytochrome c′

The construction of the plasmid for bacterial expression of *R. palustris* cytochrome c′ has been described [11]. All experiments were done with the Gln1Ala pseudo-wild-type protein. The cytochrome *c′* plasmid (Amp^r) and the cytochrome *c* maturation gene cassette pEC86 (Chl^r) [12] from L. Thöny-Meyer were co-transformed into *E. coli* BL21 Star™ cells (Invitrogen) and the protein was expressed using a previously described protocol [13]. After the cell pellets turned red, the large culture was spun down (15 min at 5000 rpm) and the protein was extracted by osmotic shock. The pellets were first resuspended in a lukewarm sucrose solution (30% sucrose, 1 mM EDTA, and 30 mM Tris·HCl, pH 8) and the suspension was centrifuged at 5000 rpm for 5-10 min. The resulting pellets were then resuspended in a cold 5 mM $MgSO_4$ solution, and this suspension was centrifuged at 8500 rpm for 40-60 min. The supernatant was collected and treated with a protease inhibitor (1 mM PMSF).

Prior to column chromatography, the crude protein extract was diluted with cold water to an ionic strength of 5 mM; and the pH was adjusted to 5.0 with concentrated acetic acid. This solution was loaded on a Fast Flow CM Sepharose column equilibrated with 5 mM NaOAc buffer at pH 5.0. The column was washed with 5 mM NaOAc buffer at pH 5.0 and the protein was eluted with a stepwise salt gradient (0 to 0.25 M NaCl). The eluted protein was concentrated, and the solution exchanged to 5 mM MES, pH 5.5 either by dialysis or repeated ultrafiltration. The protein was further purified by ion-exchange chromatography with a Mono S or HP SP Sepharose column using an FPLC system (Pharmacia). The column was equilibrated with 5 mM MES buffer at pH 5.5 and the protein was eluted with a linear salt gradient from 0 to 0.2 M NaCl in 5 mM MES buffer at pH 5.5. The protein purity was judged by the 0.19-0.21 A_{280}:A_{398} ratio and also checked with SDS gel electrophoresis and electrospray mass spectrometry. The protein concentration was determined from the known absorptivity ε_{398} of 89 $mM^{-1}cm^{-1}$.

Cyclophilin

The plasmid (Amp^r) encoding the GST fusion construct of the human cyclophilin A gene (CyP) obtained from A. H. Andreotti at Iowa State University was transformed into *E. coli* BL21 Star™ cells. The cells were grown in LB media containing 100 mg/L ampicillin at 37 °C to A_{600} 0.6. The temperature was lowered to 28 °C, and IPTG was added (final concentration of

1 mM) to induce overexpression of the fusion protein. The cells were harvested by centrifugation after 8 h of induction and lysed with lysozyme; the lysate was treated further with DNase and PMSF, and then purified on a glutathione column using a published method [14]. The GST tag was cleaved by thrombin treatment overnight (the cleavage reaction was quenched with PMSF). The mixture was again purified on a glutathione column and then by cation-exchange chromatography on an HP SP Sepharose column [15]. The CyP purity was confirmed by SDS-PAGE (single band) and ES-MS. The enzyme was purified and stored in the presence of 2 mM DTT; the reducing agent was removed with desalting columns or dialysis immediately prior to use in activity assays or refolding experiments. Concentrations of CyP were determined from absorptivity ε_{280} of 8730 $M^{-1}cm^{-1}$ [16].

The activity of CyP was assessed with a chymotrypsin-coupled chromogenic assay utilizing the substrate *N*-succinyl-Ala-Ala-Pro-Phe-*p*-nitroanilide [17]. Five concentrations of CyP ranging from 0 to 10 nM were used; reaction kinetics in each experiment were monitored by collecting 390 nm absorbance readings every 1 s for 200 s. First-order rate constants (k_{obs}) were derived by nonlinear least squares fitting of the data to a single-exponential function. The assay yielded k_{cat}/K_m of 3.6×10^6 $M^{-1}s^{-1}$ at 15 °C, confirming efficient catalysis of peptidyl-prolyl *cis-trans* isomerization by the recombinant protein. The activity is somewhat lower than that of another recombinant CyP [17]; the difference may be due to the more extended N-terminal sequence of our protein construct.

Equilibrium Unfolding

The unfolding curves were generated from CD, absorption, and fluorescence data using a standard procedure [18]. Aliquots of concentrated cyt c′ were added to pH-adjusted GuHCl solutions with gas-tight Hamilton syringes to provide a series of solutions with the same protein concentration. The samples were equilibrated at room temperature for at least 30 min before measurements. Denaturant concentrations were determined from refractive index measurements [19].

pH Titration

The titration curve was generated from cyt c′ absorption spectra at different pH values. Syringe aliquots of concentrated cyt c′ were added to a series of pH-adjusted solutions of 6 M GuHCl. Immediately after spectroscopic measurements, pH values of protein samples were double-checked with a narrow-stem electrode.

Steady-State Spectroscopic Measurements

Absorption and CD spectra were recorded with a Hewlett-Packard 8452A Diode-Array spectrophotometer and an Aviv 62ADS spectropolarimeter. Fluorescence spectra were recorded with a Jobin Yvon/SPEX Fluorolog spectrofluorimeter (λ_{ex} 290; λ_{obs} 300-370 nm).

Stopped-Flow Measurements

Protein refolding was triggered using a Bio-Logic SFM-4S stopped-flow mixer. Unfolded cyt *c*′ (3 M GuHCl, 100 mM NaOAc at pH 5) was diluted with a refolding buffer consisting of 100 mM NaOAc at pH 5 and 3 M GuHCl at pH 5. The experimental setup for fluorescence measurements has been described [10]. The sample in a 2.0 mm cuvette (FC-20, Bio-Logic) was excited with a 200-W mercury-xenon arc lamp (Hg lines picked with a 266-nm dielectric mirror) and the 355 nm luminescence was selected with a monochromator. The final protein concentrations were 10-20 μM; the mixing deadtime was ≤5 ms. Absorbance changes in a 10-mm zigzag cuvette (TC-100-15, Bio-Logic) were probed with a 75-W xenon arc lamp and detected with either a photomultiplier tube coupled to a digital oscilloscope (single-wavelength measurements) or an Ocean Optics USB2000 CCD camera (full spectra in the 300-500 nm

range). The CCD camera (integration time of 50 ms) was triggered every 100 ms by a series of pulses from a gate-delay generator. The final protein concentrations in the absorbance experiments were 3-10 μM and the mixing deadtime was ≈7 ms.

Slow Kinetics

Slow kinetics were monitored with absorption spectroscopy (190-820 nm) on a Hewlett-Packard 8452A Diode-Array spectrophotometer. Folding was triggered by manual 1:9 mixing of unfolded protein solution with the refolding buffer. The mixing deadtime was ≤30 s. The protein solution was stirred at 750 rpm in a sealed 1.0-cm quartz cuvette.

Data Analysis

Data were analyzed with SigmaPlot 2001 (SPSS Inc.) and MATLAB v. 6.5 (The Math Works, Inc). Singular value decomposition of the matrix containing the time series of absorption spectra $\mathbf{A}(\lambda_m,t_n)$ provided basis $\mathbf{U}(\lambda)$ vectors with the spectral information and the time dependence vectors $\mathbf{V}(t)$ (eq 1) [20]:

$$\mathbf{A}=\mathbf{USV}^{\mathrm{T}} \quad (1)$$

The resulting SVD components $V_i(t)$ were simultaneously fitted to a sum of exponentials yielding apparent rate constants and an amplitude matrix. The model (see **Results and Discussion**) defined the set of differential equations that are the rate laws for each of the three species; solution of these equations yielded the concentration matrix. Intermediate spectra were calculated from the experimental absorbance time series using this concentration matrix along with experimental spectra of unfolded and folded proteins.

Results and Discussion

Cyt *c′* Folding at pH 5

Previous cyt *c′* folding experiments were performed at neutral pH. The shift to pH 5 was driven by the desire to eliminate effects owing to misligation (a major folding trap for cytochrome *c*) [21]. Although His misligation is not a factor for cyt *c′* (the native axial ligand His117 is the only His), the N-terminal amino group as well as sidechains of some of the Lys residues can still coordinate to the heme in the unfolded protein at pH 7 [22,23]. A pH titration of guanidine hydrochloride (GuHCl)-denatured cyt *c′* (Fig. 2) yielded a midpoint pH of 7.7±0.1, consistent with the pK_a value of either a heme-bound water or a protein amino group [22]. Although amino-group misligated species would constitute only a fraction of the denatured ensemble at pH 7, they can still slow protein refolding and contribute to heterogeneous kinetics.

Equilibrium unfolding of cyt *c′* has been monitored by three different spectroscopic techniques: circular dichroism (CD), absorbance, and fluorescence (Fig. 3). All three methods indicate a cooperative unfolding transition with a midpoint of 1.9±0.1 M GuHCl. The thermodynamic stability toward GuHCl denaturation at pH 5 is essentially the same as at pH 7 [10]. At both pH values folding is more than 90% reversible.

Refolding Kinetics

The kinetics of refolding (rates and amplitudes of the burst signal) depend on the final GuHCl concentration (Fig. 4). In general, two rate constants differing by an order of magnitude (k_1 and k_2) are needed to describe the refolding kinetics in the time regime <5 s. The exception is Trp72 fluorescence at GuHCl concentrations higher than 0.6 M; these kinetics are adequately described by a single exponential function. Both absorbance and fluorescence measurements give similar rate constants k_1 for the dominant faster phase (Fig. 4c). However, the two techniques reveal differences at longer timescales. While fluorescence-detected folding is

complete in a few seconds, very small (<10% of the total signal) but detectable absorbance changes persist for minutes (Fig. 5). During this slow transformation the Soret band decreases in intensity and broadens slightly.

The fluorescence burst signal (Fig. 4d) is consistent with compaction of the protein ensemble. Analysis of Trp-to-heme distance distributions has demonstrated that the compact structures formed at this stage of folding are not native-like [2]. Apparently there is relatively late assembly of the large loop between helices II and III and possibly even of the entire II-III-IV bundle. The compact intermediates clearly lack some of the tertiary contacts found in the native structure.

Absorption spectra provide additional information about the properties of these intermediates and the overall cyt *c′* folding process. Heme spectra are sensitive to changes in environment due to ligand substitution, solvent exposure, and the surrounding polypeptide. In studies of intricate reactions, such as protein folding, measurements of full spectral changes (Figs. 6 and 7a) provide additional information not found in single-wavelength measurements (Fig. 4a). Nevertheless, the single-wavelength data already point to the complexity of cyt *c′* refolding. At lower GuHCl concentrations, that favor polypeptide collapse, the rate constants k_1 are different at 372 and 400 nm (Fig. 4a), suggesting that the observed folding transformation is not a simple two-state process.

We have analyzed transient absorption spectra of cyt *c′* in the entire range from 300 to 500 nm. The folded protein has a broad Soret band characteristic of a five-coordinate heme (Fig. 6c); the unusual shape of this band has been attributed to a quantum mechanical mixture of intermediate- $(S={}^3/_2)$ and high- $(S={}^5/_2)$ spin states [24]. The absorption spectrum of the unfolded protein at pH 5 (Fig. 6a) shows features of a six-coordinate high-spin heme, similar to those of the Met80Ala mutant of cytochrome *c* [25]. The axial ligands are His117 and a weak-field donor (presumably water). A series of transient absorption spectra recorded during refolding (Fig. 7a) document a decrease and broadening of the Soret band consistent with formation of the native heme environment, but they do not provide a clear indication of the presence of a spectroscopically distinct intermediate. In fact, the entire series can be satisfactorily described as a linear combination of the spectra of unfolded and folded proteins, arguably the sign of a simple two-state refolding process. However, the time evolution of spectral amplitudes deviates from monoexponential behavior (Fig. 7c), suggesting that the refolding process is more complex.

We have employed singular-value decomposition (SVD) to evaluate the minimal number of distinct species contributing to the absorbance/time series (see **Materials and Methods** for details). Analysis of the kinetics data at 1.2 M GuHCl (Fig. 7a) reveals two significant components with singular values s_1=94.4 and s_2=3.9. The s_1/s_2 ratio indicates that the spectral changes are dominated by the first component. Simultaneous fitting of the two time dependence vectors $V(t)$ yielded apparent rate constants k_1=3.1 s^{-1} and k_2=0.4 s^{-1}. As seen from the extracted basis spectra (Fig. 7b), there is no distinct spectral shift but rather just a decrease and broadening of the Soret band during refolding. The SVD analysis suggests that unfolded, folded, and an intermediate species should be included to account for the absorbance kinetics.

Catalysis of Refolding by Cyclophilin

Proline isomerization is a well-known contributor to slow refolding [26]. There are proline residues at positions 21, 52, 56, and 69 in the cyt *c′* sequence, all of which have *trans* imide bonds in the native structure. Thus any nonnative *cis* isomers in the unfolded ensemble must undergo *cis-trans* isomerization during folding.

The prolyl *cis-trans* isomerase cyclophilin often catalyzes slow refolding reactions [16, 27-30]. In cyt *c′*, we find that the rate of the faster folding phase is unaffected by the presence of cyclophilin in the refolding buffer, but the slower phase ($k_2 \approx 1\ s^{-1}$) disappears completely (Fig. 8). The slowest (minutes-long, k_{min}) kinetics phase does not respond to the addition of cyclophilin: similar absorbance changes are observed with and without the enzyme. Other slow processes, such as intermolecular aggregation, could be responsible for the observed signal, although certain of the prolyl peptide bonds might be inaccessible to the enzyme even at moderate denaturant concentrations (0.6 M GuHCl) [16].

Mechanistic Model

Even in the absence of misligation, the cyt *c′* four-helix bundle folds slowly. Turning now to the mechanism, we emphasize that our model-independent SVD analysis of the time-resolved absorbance data compellingly demonstrates that refolding deviates from a two-state process, as heme absorption kinetics are biexponential with three distinct species contributing to the spectral change. In addition, the results of our cyclophilin experiments suggest that the slower phase arises from *cis-trans* prolyl isomerization.

The simplest mechanism consistent with these data is shown in Scheme 1. In intermediate I_c, one or more prolines are assumed to have nonnative *cis* imide bonds. The refolding of I_c is rate-limited by prolyl *cis-trans* isomerization with a microscopic rate constant k_{2c} equal to the smaller apparent rate constant k_2. The higher apparent rate constant k_1 is the sum of k_{1t} and k_{1c}. Employing this model, we extracted the spectrum of the putative intermediate I_c from the experimental absorbance time series (Fig. 9). For all different values of k_{1t}, the spectrum of I_c closely resembles that of the unfolded protein, suggesting that the heme is not fully protected in this species. On the other hand, the Trp72 fluorescence is largely quenched after just one second of refolding (Fig. 7d), indicating that the I_c species is compact, with a short Trp72-to-heme distance.

It is difficult to assign the slow kinetics phase to a specific proline residue. Among the four prolines, however, Pro21 is a particularly strong candidate. Compared to the three other prolines (two in the large interhelical loop, Pro56 and Pro69, and one at the very end of a helix, Pro 52), this residue occupies a unique position in the middle of a helix. The Pro21-induced bend [7] directs some of the interactions of helix I with helix II as well as with the heme. Nonnative positioning of this helix due to a Lys20-Pro21 *cis*-geometry could lead to increased solvent exposure of the heme, in accord with the spectral data.

We emphasize that the extracted spectra of I_c strongly depend on the kinetics model. We have conservatively chosen the simplest scheme consistent with our SVD, fluorescence, and cyclophilin catalysis data. Theoretical studies, as well as recent experimental work, suggest that protein folding may not be a simple two- or even three-state process, but rather involve a large number of alternative pathways with many different intermediates [31-34]. Indeed, the extracted I_c spectra resemble those of a mixture of components and not that of a unique species. Our earlier fluorescence energy transfer experiments indicated substantial heterogeneity of the polypeptide ensemble in the first few milliseconds of refolding [2]. However, a question remains about the extent of such heterogeneity during the later stages, when prolyl *cis-trans* isomerization is taking place. The absorption data alone do not allow us to identify any other species, so introduction of additional complexity to the model is unwarranted at this point.

Conclusions

Our refolding data at pH 5 clearly demonstrate that polypeptide dynamics rather than ligand substitution reactions slow cyt *c′* refolding. Encapsulation of a five-coordinate heme is associated with large absorbance changes during formation of the native structure. The SVD

analysis provides important information about the complexity of the reaction, revealing that it is not a two-state process. Rate acceleration upon addition of cyclophilin points to a prominent role for *cis-trans* prolyl isomerization during assembly of the four-helix bundle; specifically, it is likely that a nonnative Pro21 configuration interferes with the formation of the native heme environment in the protein. We conclude that *cis*-configured prolines are responsible for some of the topological and energetic frustration of the collapsed polypeptide ensemble [2].

Acknowledgements

We thank Professor Amy H. Andreotti for providing human cyclophilin plasmid and Binghai Ling for screening bacterial colonies for cyt *c′* expression. Our work was supported by NIH (GM068461 to J.R.W.), the Ellison Medical Foundation (Senior Scholar Award in Aging to H.B.G.), the Caltech SURF program (Mr. And Mrs. Samuel Krown fellowship to Z.Z.), and the Japan Society for the Promotion of Science for Young Scientists (Research Fellowship to T. K.).

References

1. Kamtekar S, Hecht MH. FASEB 1995;9:1013–1022.
2. Kimura T, Lee JC, Gray HB, Winkler JR. Proc Natl Acad Sci USA 2007;104:117–122. [PubMed: 17179212]
3. Faraone-Mennella J, Gray HB, Winkler JR. Proc Natl Acad Sci USA 2005;102:6315–6319. [PubMed: 15843463]
4. Wittung-Stafshede P, Lee JC, Winkler JR, Gray HB. Proc Natl Acad Sci USA 1999;96:6587–6590. [PubMed: 10359755]
5. Kragelund BB, Osmark P, Neergaard TB, Schiødt J, Kristiansen K, Knudsen J, Poulsen FM. Nature Struct Biol 1999;6:594–601. [PubMed: 10360367]
6. Huang GS, Oas TG. Proc Natl Acad Sci USA 1995;92:6878–6882. [PubMed: 7624336]
7. Shibata N, Iba S, Misaki S, Meyer TE, Bartsch RG, Cusanovich MA, Morimoto Y, Higuchi Y, Yasuoka N. J Mol Biol 1998;284:751–760. [PubMed: 9826513]
8. Lee JC, Gray HB, Winkler JR. Proc Natl Acad Sci USA 2001;98:7760–7764. [PubMed: 11438728]
9. Tezcan FA, Winkler JR, Gray HB. J Am Chem Soc 1998;120:13383–13388.
10. Lee JC, Engman KC, Tezcan FA, Gray HB, Winkler JR. Proc Natl Acad Sci USA 2002;99:14778–14782. [PubMed: 12407175]
11. McGuirl MA, Lee JC, Lyubovitsky JG, Thanyakoop C, Richards JH, Gray HB, Winkler JR. Biochim Biophys Acta 2003;1619:23–28. [PubMed: 12495812]
12. Arslan E, Schulz H, Zufferey R, Künzler P, Thöny-Meyer L. Biochem Biophys Res Commun 1998;251:744–747. [PubMed: 9790980]
13. Pletneva EV, Gray HB, Winkler JR. J Mol Biol 2005;345:855–867. [PubMed: 15588831]
14. Brazin KN, Fulton DB, Andreotti AH. J Mol Biol 2000;302:607–623. [PubMed: 10986122]
15. Yoo S, Myszka DG, Yeh C, McMurray M, Hill CP, Sundquist WI. J Mol Biol 1997;269:780–795. [PubMed: 9223641]
16. Veeraraghavan S, Nall BT. Biochemistry 1994;33:687–692. [PubMed: 8292595]
17. Liu J, Albers MW, Chen CM, Schreiber SL, Walsh CT. Proc Natl Acad Sci USA 1990;87:2304–2308. [PubMed: 2179953]
18. Creighton, TF. Protein Structure: a Practical Approach. Oxford University Press; New York: 1997.
19. Nozaki Y. Meth Enzymol 1972;26:43–50. [PubMed: 4680720]
20. Van Eps N, Szundi I, Einarsdottir O. Biochemistry 2003;42:5065–5073. [PubMed: 12718550]
21. Elöve G, Bhuyan AK, Roder H. Biochemistry 1994;33:6925–6935. [PubMed: 8204626]
22. Hammack BN, Godbole S, Bowler BE. J Mol Biol 1998;275:719–724. [PubMed: 9480763]
23. Smith CR, Wandschneider E, Bowler BE. Biochemistry 2003;42:2174–2184. [PubMed: 12590607]
24. Weber P. Biochemistry 1982;21:5116–5119. [PubMed: 6293536]
25. Lu Y, Casimiro DR, Bren KL, Richards JH, Gray HB. Proc Natl Acad Sci USA 1993;90:11456–11459. [PubMed: 8265573]

26. Nall BT. Biochemistry 1983;22:1423–1429. [PubMed: 6301548]
27. Lang K, Schmid FX, Fischer G. Nature 1987;329:268–270. [PubMed: 3306408]
28. Pappenberger G, Bachmann A, Müller R, Hüseyin A, Engels JW, Kiefhaber T. J Mol Biol 2003;326:235–246. [PubMed: 12547205]
29. Kern G, Kern D, Schmid FX, Fischer G. J Biol Chem 1995;270:740–745. [PubMed: 7822304]
30. Wu Y, Matthews CR. J Mol Biol 2002;323:309–325. [PubMed: 12381323]
31. Onuchic JN, Luthey-Schulten Z, Wolynes PG. Annu Rev Phys Chem 1997;48:545–600. [PubMed: 9348663]
32. Dobson CM, Sali A, Karplus M. Angew Chem Int Ed Eng 1998;37:868–893.
33. Pletneva EV, Gray HB, Winkler JR. Proc Natl Acad Sci USA 2005;102:18397–18402. [PubMed: 16344477]
34. Zhuang X, Rief M. Curr Opin Struct Biol 2003;13:88–97. [PubMed: 12581665]
35. Hammack BN, Smith CR, Bowler BE. J Mol Biol 2001;311:1091–1104. [PubMed: 11531342]

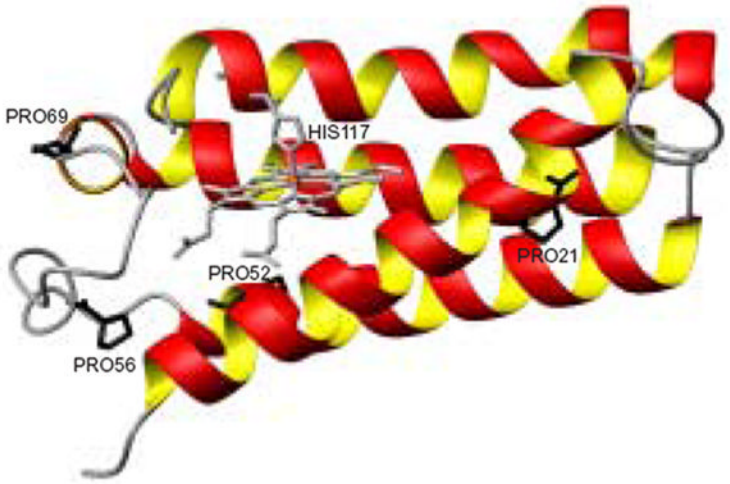

Fig. 1.
Structure of *R. palustris* cyt *c′* (1A7V) [7] showing the heme ligand (His117) and four prolines (21, 52, 56, and 69).

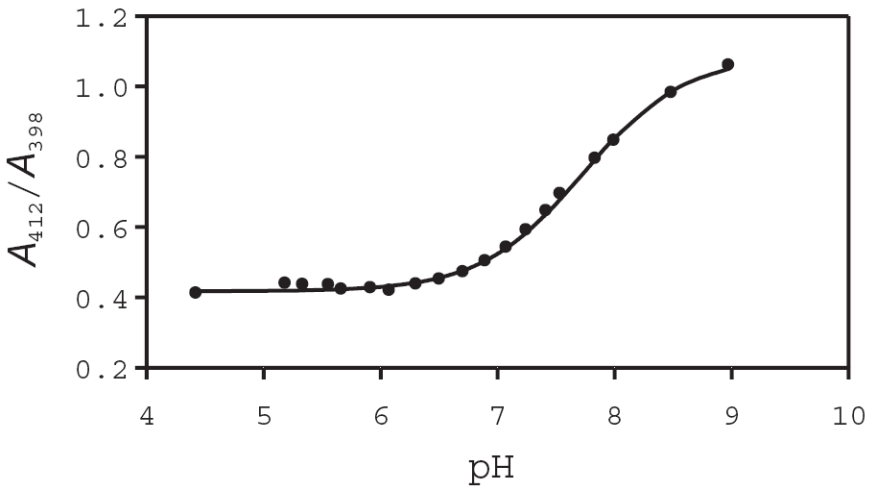

Fig. 2.

Absorption changes during the pH titration of pseudo-wild-type (Gln1Ala) *R. palustris* cyt *c′* in 6 M GuHCl. The solid line is the Henderson-Hasselbalch fit [35] with pK_a 7.7±0.1 (*n*=0.99 ±0.05).

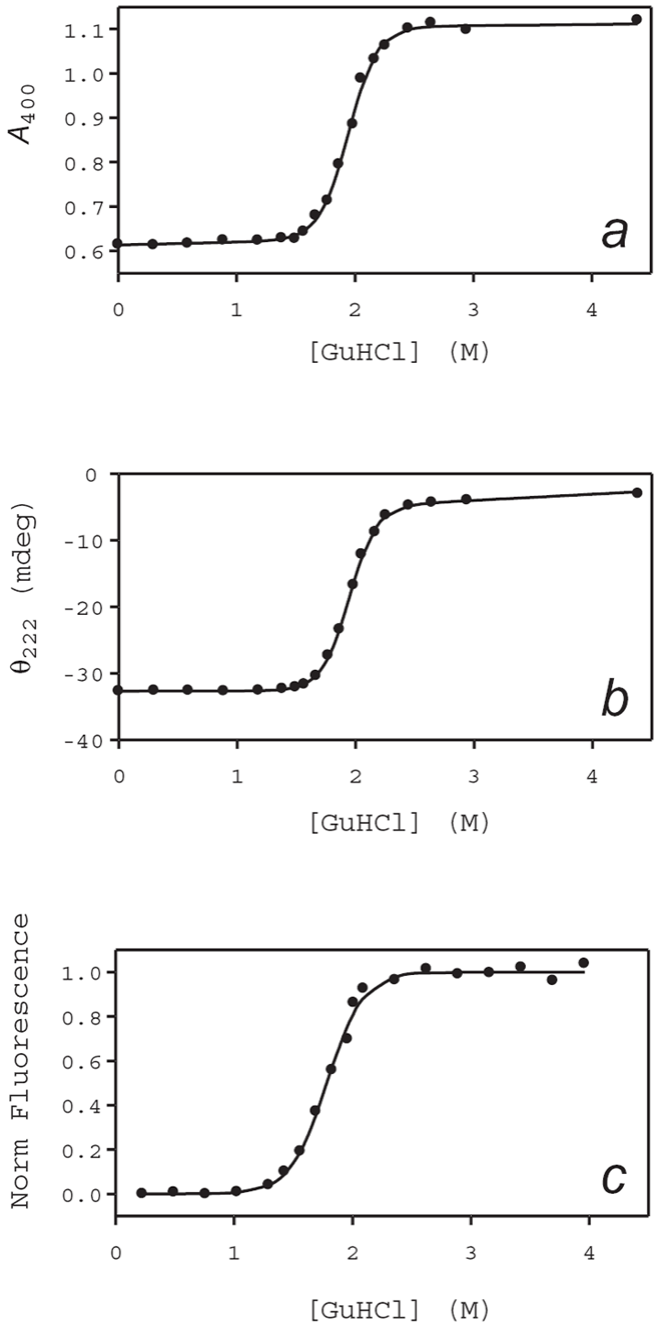

Fig. 3.

Unfolding curves for Gln1Ala cyt *c′* at pH 5.0 from (a) heme absorption, (b) circular dichroism, and (c) tryptophan fluorescence measurements. The solid lines are fitsto a two-state unfolding model.

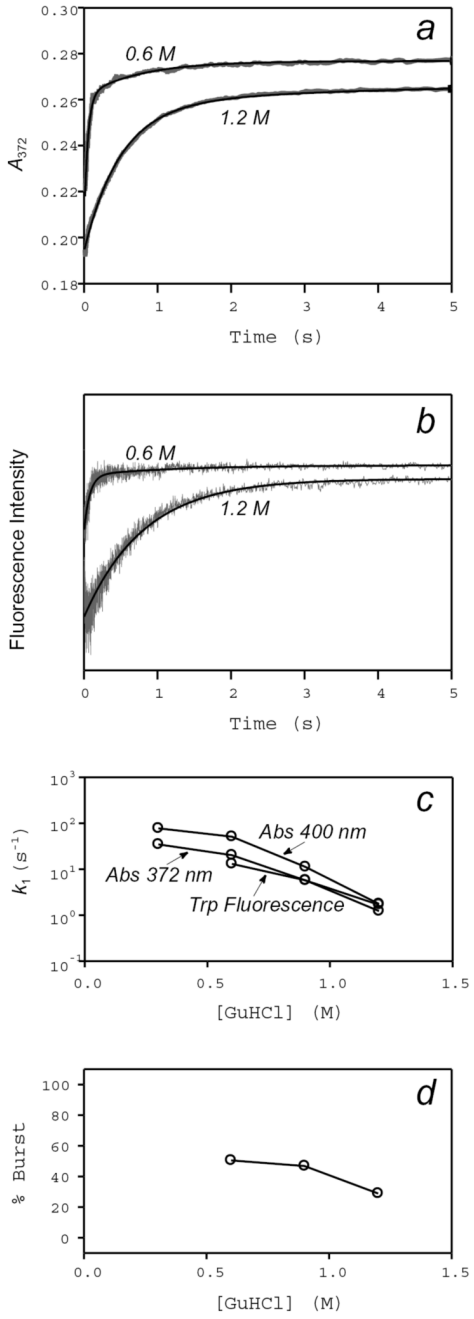

Fig. 4.

Stopped-flow measurements of the refolding kinetics of Gln1Ala cyt *c*′ at pH 5.0. (a) Absorbance changes at 372 nm: *upper curve*, $[GuHCl]_{final}$=0.6 M; *lower curve*, $[GuHCl]_{final}$=1.2 M. (b) Change in fluorescence intensity at 355 nm: *upper curve*, $[GuHCl]_{final}$=0.6 M; *lower curve*, $[GuHCl]_{final}$=1.2 M. (c) Larger rate constant (k_1) from measurements of absorbance changes at 372 nm (increase in the folded protein population), 400 nm (decrease in the unfolded protein population), and of Trp72 fluorescence as a function of $[GuHCl]_{final}$. (d) Amplitude of the Trp72 burst phase (<5 ms) as a function of $[GuHCl]_{final}$.

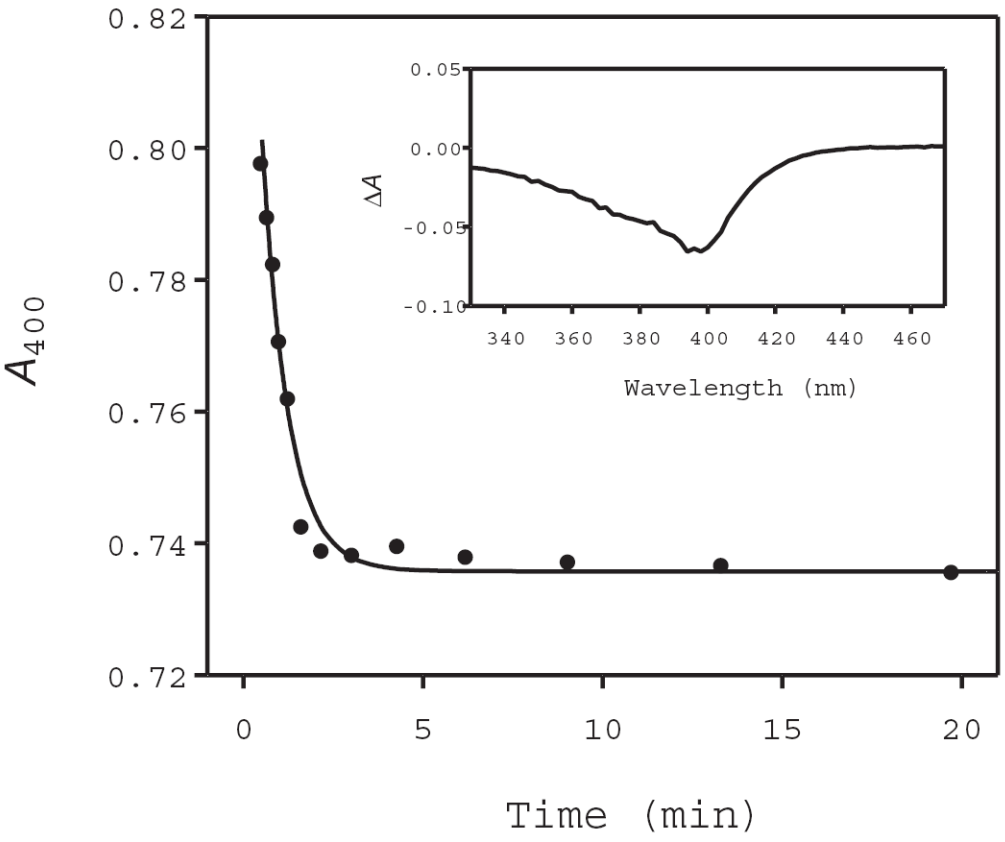

Fig. 5.

Slow absorbance changes during refolding of Gln1Ala cyt *c′* at pH 5.0 from 3.0 M into 1.2 M GuHCl. *Inset*: difference spectrum between 50 and 0.5 min.

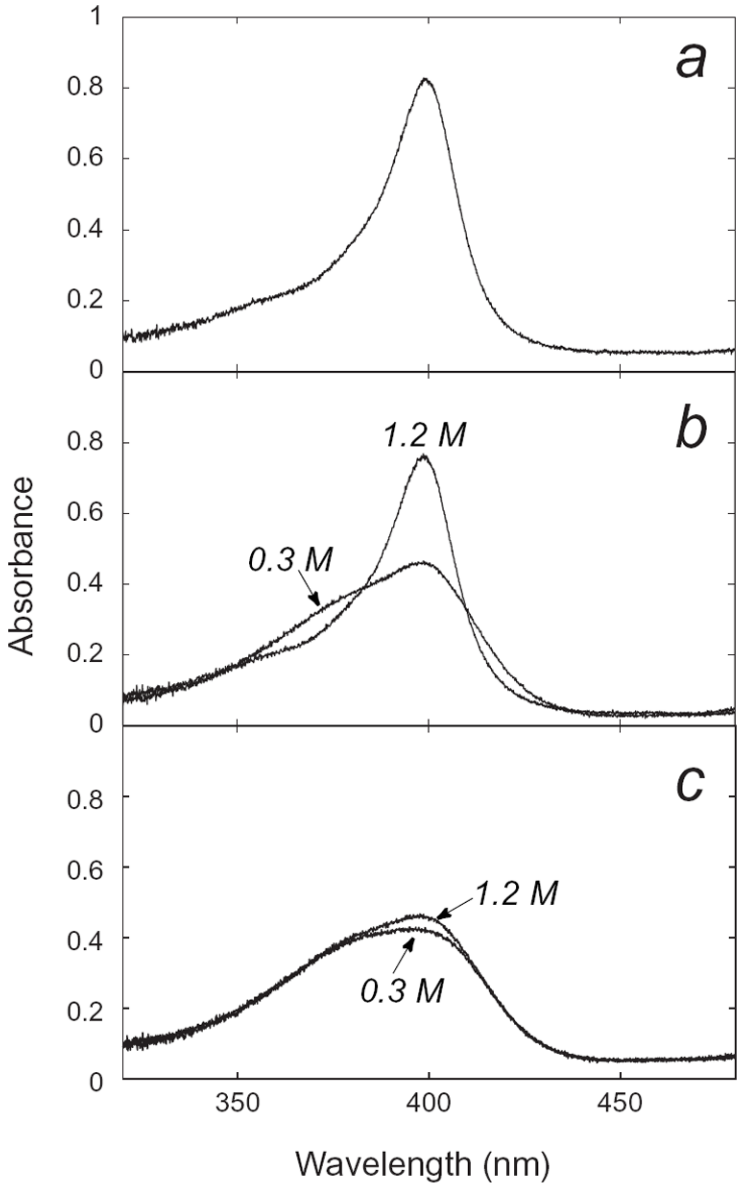

Fig. 6.

Absorption spectra of Gln1Ala cyt *c*′ at pH 5.0: (a) unfolded in 3.0 M GuHCl; (b) 50 ms after initiation of refolding from 3.0 M into 0.3 and 1.2 M GuHCl; (c) 10 s afterinitiation of refolding from 3.0 M into 0.3 and 1.2 M GuHCl.

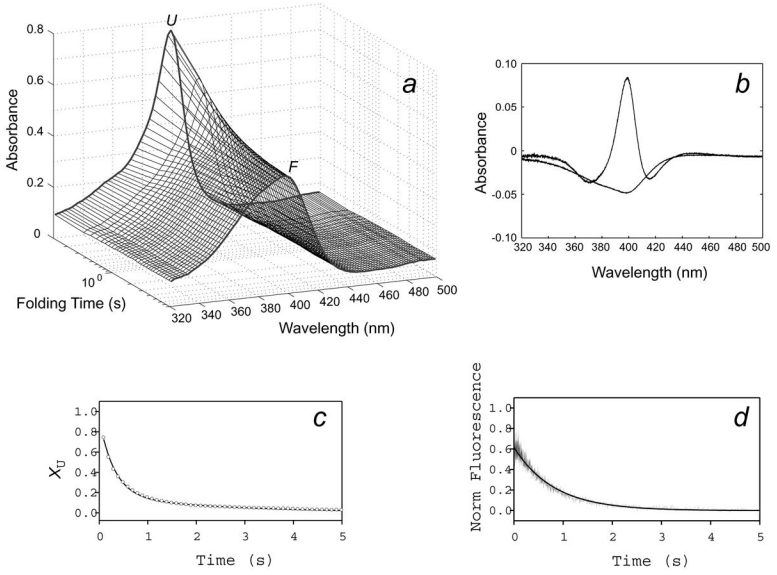

Fig. 7.

(a) Time-resolved absorption spectra of Gln1Ala cyt *c*′ during refolding at pH 5.0 from 3.0 M into 1.2 M GuHCl. (b) Basis spectra from SVD analysis of the data. (c) Fraction of the unfolded protein from a two-state deconvolution of the spectral series (the solid line is a fit to a biexponential function (k_1=3.1 s^{-1} and k_2=0.4 s^{-1}; see text). (d) Trp72 kinetics and the corresponding fit (k=1.2 s^{-1}) under the same refolding conditions.

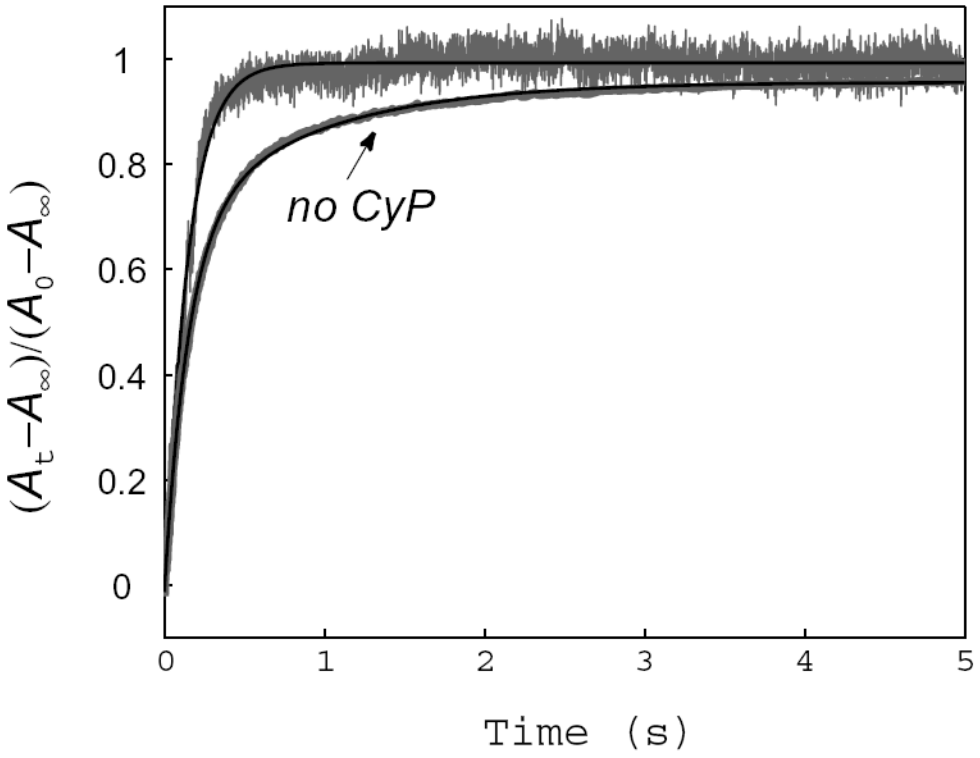

Fig. 8.

Kinetics of Gln1Ala cyt *c*′ refolding monitored by absorbance changes at 372 nm with and without recombinant cyclophilin. Refolding conditions: 0.6 M GuHCl; 100 mM HEPES buffer; pH 7; 18 °C. The refolding experiments were done at neutral pH to avoid any decrease in enzymatic activity at pH 5. Moderate concentrations of the denaturant GuHCl (<0.7 M) keep the enzyme active and assist in the catalysis of folded substrates [16]. Rate constants (relative amplitudes of the fits): *lower trace* (no CyP), biexponential, k_1=6.8 s^{-1}, k_2=1.2 s^{-1} (30%); *upper trace* (20 μM CyP), monoexponential, k=7.0 s^{-1}.

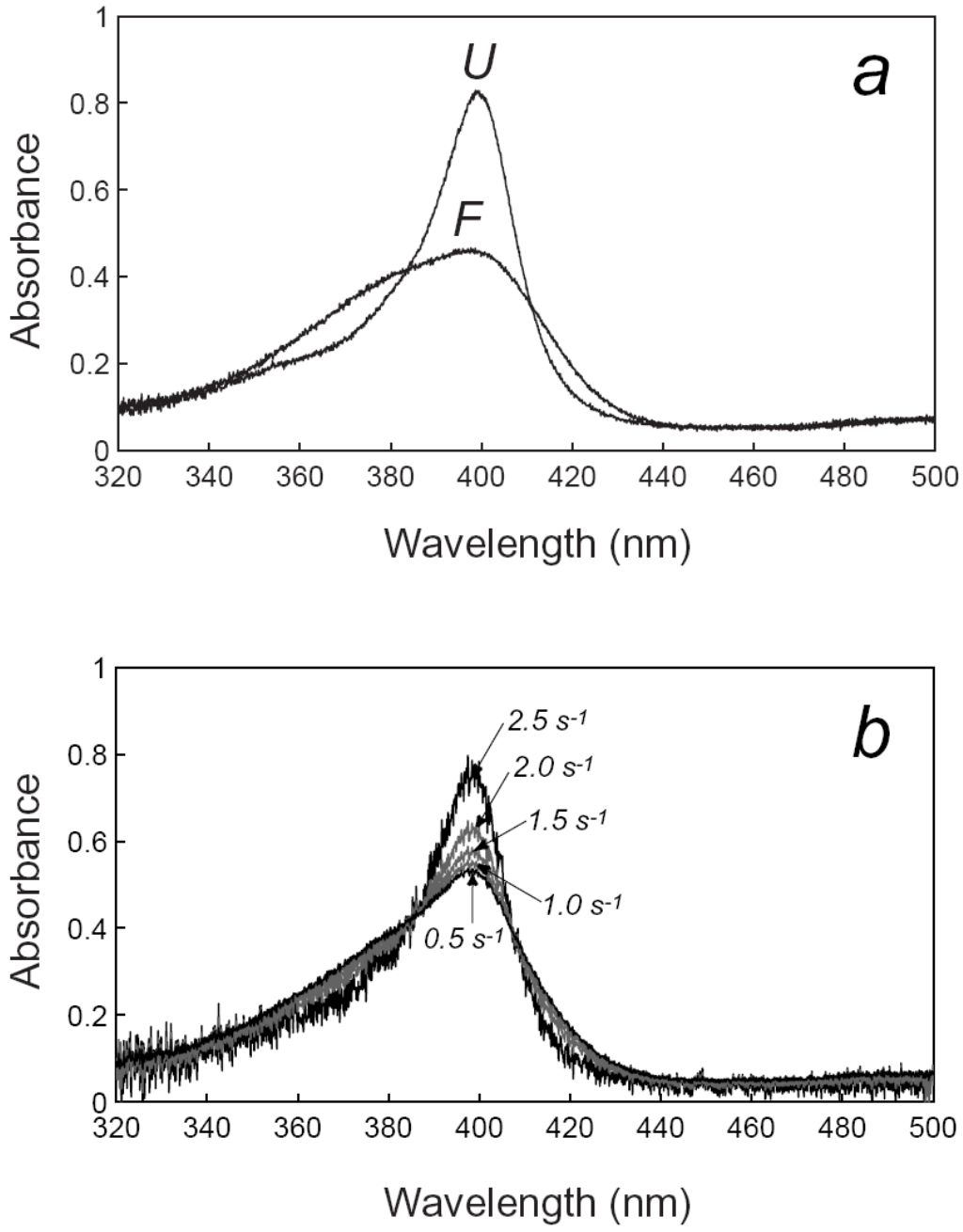

Fig. 9.

Calculations of I_c spectra (mechanistic model, Scheme 1: (a) spectra of unfolded and folded protein from the absorption time series in Fig. 7; (b) extracted spectra for intermediate I_c for different values of the microscopic rate constant k_{1t} (indicated on the graph). Experimentally determined apparent rate constants define values of the microscopic constants k_{1c} and k_{2c}, see text.

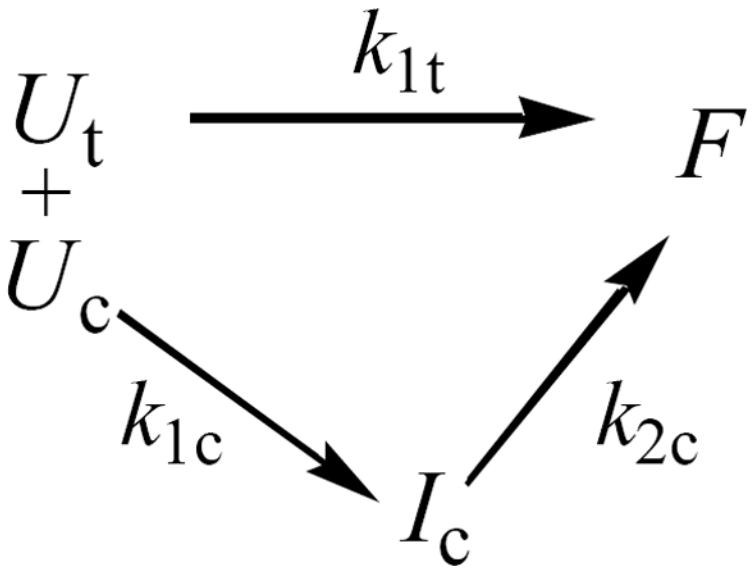

Scheme 1.